Effect of transverse magnetic fields on dose distribution and RBE of photon beams: comparing PENELOPE and EGS4 Monte Carlo codes

IOP PUBLISHING PHYSICS IN MEDICINE AND BIOLOGY

Phys. Med. Biol. **53** (2008) 5123–5137 doi:10.1088/0031-9155/53/18/018

Effect of transverse magnetic fields on dose distribution and RBE of photon beams: comparing PENELOPE and EGS4 Monte Carlo codes

H Nettelbeck, G J Takacs and A B Rosenfeld

Centre for Medical Radiation Physics, University of Wollongong, Australia

E-mail: hn06@uow.edu.au

Received 27 March 2008, in final form 25 July 2008
Published 22 August 2008
Online at stacks.iop.org/PMB/53/5123

Abstract

The application of a strong transverse magnetic field to a volume undergoing irradiation by a photon beam can produce localized regions of dose enhancement and dose reduction. This study uses the PENELOPE Monte Carlo code to investigate the effect of a slice of uniform transverse magnetic field on a photon beam using different magnetic field strengths and photon beam energies. The maximum and minimum dose yields obtained in the regions of dose enhancement and dose reduction are compared to those obtained with the EGS4 Monte Carlo code in a study by Li *et al* (2001), who investigated the effect of a slice of uniform transverse magnetic field (1 to 20 Tesla) applied to high-energy photon beams. PENELOPE simulations yielded maximum dose enhancements and dose reductions as much as 111% and 77%, respectively, where most results were within 6% of the EGS4 result. Further PENELOPE simulations were performed with the Sheikh-Bagheri and Rogers (2002) input spectra for 6, 10 and 15 MV photon beams, yielding results within 4% of those obtained with the Mohan *et al* (1985) spectra. Small discrepancies between a few of the EGS4 and PENELOPE results prompted an investigation into the influence of the PENELOPE elastic scattering parameters C_1 and C_2 and low-energy electron and photon transport cut-offs. Repeating the simulations with smaller scoring bins improved the resolution of the regions of dose enhancement and dose reduction, especially near the magnetic field boundaries where the dose deposition can abruptly increase or decrease. This study also investigates the effect of a magnetic field on the low-energy electron spectrum that may correspond to a change in the radiobiological effectiveness (RBE). Simulations show that the increase in dose is achieved predominantly through the lower energy electron population.

1. Introduction

Since the advent of radiotherapy as a means of tumour control an ongoing challenge has been to reduce the radiation dose to normal tissue. Conformal radiotherapy, intensity modulated radiotherapy and brachytherapy are three physical methods in current use. Magneto-therapy, or the use of magnetic fields to produce a favourable redistribution of dose, despite being suggested over half a century ago, is still not in use. This is primarily due to the practical difficulty of applying magnetic fields of sufficient strength to bring about a significant alteration of the dose deposition. A secondary consideration is the incorporation of the effects of the magnetic fields on the dose distribution into the treatment planning process. A third consideration is the potential for any change in radiobiological effectiveness of the radiation through physical, chemical or biological means.

Changes in technology mean that the ability to apply sufficiently strong magnetic fields will soon be at hand. Therefore it is desirable to extend earlier studies to allow further progress to be made in the second and third areas referred to above. This paper constitutes another step on that path.

The concept of applying magnetic fields to alter the dose deposition of scattered electrons from radiotherapy beams was suggested by Bostick in 1950. He proposed that a longitudinal magnetic field applied during electron beam therapy would reduce the lateral scattering of secondary electrons, thereby reducing the penumbral broadening of the beam with depth (Bostick 1950). Since then a number of researchers have performed Monte Carlo studies to explore how transverse and longitudinal magnetic fields can be used to tailor the dose distribution from radiotherapy beams (Shih 1975, Whitmire and Bernard 1977a, 1977b, Bielajew 1993, Nardi and Barnea 1999, Jette 2000a, 2000b, Lee and Ma 2000, Li *et al* 2001, Litzenberg *et al* 2001, Raaymakers *et al* 2004, Chen *et al* 2005, Raaijmakers *et al* 2007, Kirkby *et al* 2008).

An electron travelling in a magnetic field experiences a Lorentz-force which bends its trajectory, between scattering events, into a helical-shaped path. The radius of curvature depends on the electron's energy and the strength of the external magnetic field in which it is travelling. The entire trajectory of an electron will not be a perfect helical shape due to scattering. The mean free path of an electron between scattering events is also strongly energy dependent. Naively, one might expect to see an effect of the magnetic field on the dose deposition only if these two characteristic lengths are comparable in size. We will see later that an effect exists even when the radius of curvature is orders of magnitude larger than the mean free path. This occurs because of the large number of interactions that an electron needs to undergo before its trajectory is significantly altered.

Studies concentrating on the alteration of dose deposition with transverse magnetic fields began in 1975 with a Monte Carlo study by Shih (1975), who found a 6 T transverse magnetic field applied to a 70 MeV electron beam reduced the lateral spread of electrons, forming a localized maximum dose region at the end of their range analogous to the well-known 'Bragg peak'. Since then, a number of studies have investigated the dose redistribution from applying transverse magnetic fields to radiotherapy beams. Whitmire and Bernard (1977a, 1977b) measured surface dose reductions of up to 40% in polystyrene and cork phantoms when magnetic fields of 0.9 to 1.8 T were applied to betatron accelerator energies of 10–45 MeV. In a Monte Carlo study by Nardi and Barnea (1999), up to 50% reduction in the surface to peak dose (a ratio used to monitor skin sparing) was obtained with a 3 T uniform field applied to a 15 MeV electron beam beyond 4 cm depth in tissue. A subsequent Monte Carlo study by Lee and Ma (2000) also showed that transverse magnetic fields applied to

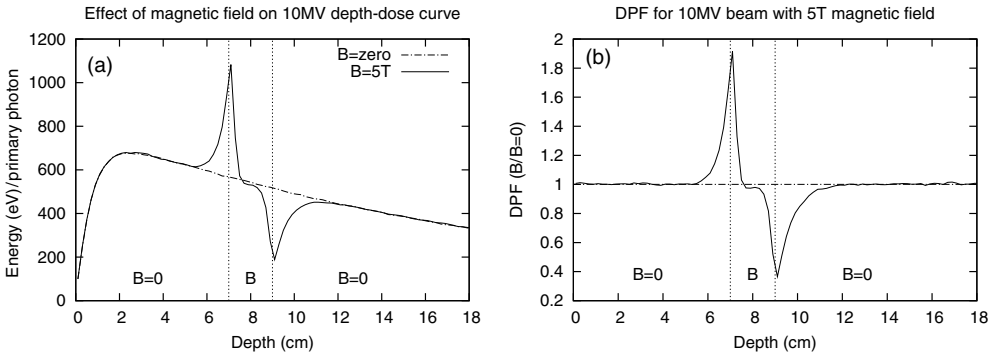

Figure 1. The effect of a slice of 5 T transverse magnetic field (7 to 9 cm depth) on the (a) depth-dose and (b) dose perturbation factor (DPF) of a 10 MV beam. The magnetic field direction points out of the page.

electron beams can significantly reduce the peak to surface dose and produce a steeper dose fall-off in the maximum dose.

Fewer studies have investigated the effect of magnetic fields on the dose distribution from photon beams. Recognizing this gap in the literature, Jette (2000b) performed Monte Carlo simulations to study changes in the dose distribution from 15, 30 and 45 MV beams when non-uniform transverse magnetic fields of up to 5 T (central strength) were applied. For all three beams, a 2 T field produced a significant enhancement in the maximum dose and a slightly larger enhancement with 3 T, where these regions of dose enhancement were immediately followed by a region of dose reduction. Stronger magnetic fields yielded a further enhancement in the maximum dose only with the 45 MV beam. Localized regions of dose enhancement and dose reduction were also observed by Li *et al* (2001) in a Monte Carlo study with EGS4 investigating the effect of transverse magnetic fields on the dose distribution from photon beams, using different strength magnetic fields (1 to 20 T) and photon beam energies (Co^{60}, 6, 10, 15, 24 and 50 MV). The slice of uniform transverse magnetic field was applied between 7 and 9 cm depth in a water phantom, and zero magnetic field was applied to the remainder of the volume. The application of different strength magnetic fields to a 15 MV beam yielded dose enhancements and dose reductions of up to 97% and 79%, respectively, which were obtained with a 5 T field. Li *et al* (2001) also studied the effect of photon beam energy on the dose distribution from Co^{60}, 6, 10, 15, 24 and 50 MV photon beams with a 5 T magnetic field and observed an increase in the maximum dose and a reduction in the minimum dose when the beam energy was increased. Li *et al* (2001) quantifies this dose perturbation effect by calculating a dose perturbation factor (DPF) which is a ratio of dose obtained with magnetic field to that obtained without magnetic field as a function of depth (along the axis of the beam), where a DPF < 1.0 is a dose reduction and a DPF > 1.0 is a dose enhancement.

Localized regions of dose enhancement and dose reduction could benefit the treatment of tumours near radiation-sensitive structures by aligning the region of dose enhancement with the tumour volume and the region of dose reduction with the critical structure. This is illustrated in figure 1 with Monte Carlo PENELOPE simulation of the effect of a slice of 5 T transverse magnetic field, perpendicular to incident beam direction, on the depth-dose and DPF of a 10 MV beam.

Whilst the effect of a magnetic field on the dose distribution has been examined, and the potential for magnetic fields to alter the relative biological effectiveness has been mentioned

(Whitmire and Bernard 1977a, Paliwal *et al* 1978, Bielajew 1993, Chen *et al* 2005), absent from the literature is a study of the effect of magnetic fields on the electron distribution from high-energy photon beams and any related change to their radiobiological effectiveness. The implementation of magnetic fields into radiotherapy has become practically feasible with the recent development of an integrated 1.5 T MRI scanner and 6 MV linear accelerator for soft-tissue tumour imaging, position verification and treatment monitoring in image-guided radiotherapy (Raaymakers *et al* 2004, Raaijmakers *et al* 2005, 2007). Studies have been performed on the system to investigate any changes in the dose deposition from the 6 MV beam due to the presence of a magnetic field. Monte Carlo simulation and physical measurements have verified that the application of a 1.1 and 1.5 T transverse magnetic field can alter the depth of maximum dose and produce asymmetric central dose profiles, where these minor changes could be accounted for in treatment planning (Raaymakers *et al* 2004). A subsequent study by Raaijmakers *et al* (2007) found that a 1.5 T transverse magnetic field could reduce the dose build-up distance. These studies did not mention the effect of a magnetic field on the electron distribution (spectrum), and subsequently, possible changes in their radiobiological effectiveness which may be an important consideration in the treatment planning process. The linear energy transfer (LET), or rate of energy loss, of an electron is known to increase with decreasing energy where an increase in LET corresponds to an increase in radiobiological effectiveness (RBE). The short-range of these low-energy electrons increases their probability of inducing lethal damage to the DNA of cells via strand breaks. For example, a 20 keV electron has a 9 μm range in tissue which is roughly the diameter of a typical human cell.

The present work uses Monte Carlo PENELOPE simulation to investigate the effect of a magnetic field on dosimetric quantities, such as the low-energy electron distribution of a 15 MV photon beam, that are not amenable to physical measurement. A comparative study of the dose distribution obtained with PENELOPE to that obtained with EGS4 in a study by Li *et al* (2001) is used to benchmark PENELOPE's charged particle transport algorithm in applications involving static electromagnetic fields. An extension of the study includes investigation of the optimal width of the magnetic field and depth at which it is applied to achieve maximum therapeutic benefit. It also investigates the potential for transverse magnetic fields to influence RBE through a change in the low-energy secondary electron spectrum.

2. Materials and methods

PENELOPE is a general-purpose Monte Carlo code used for the simulation of coupled electron-photon transport. The accurate low-energy electron and photon cross-sections gives PENELOPE a superiority over other Monte Carlo codes for applications involving low-energy transport. For example, PENELOPE can transport electrons and photons with energies as low as 100 eV (Salvat *et al* 2003) which is much lower than the EGS4 low-energy transport cut-off of 1 keV for photons and tens of keV for charged particles (Nelson *et al* 1985). Another key difference between EGS4 and PENELOPE lies in the electron transport algorithms. Whilst both codes still utilize condensed history methods the implementation of that method varies significantly between the codes. Hence, it is logical to examine if the two codes make similar predictions about the effect of a magnetic field on the dose deposition. Another difference between the codes is in the algorithm provided for incorporating the effects of a magnetic field on the electron transport. The algorithm in PENELOPE provides for exact tracking in a uniform magnetic field.

The present work compares the dose enhancement and dose reduction obtained with PENELOPE and EGS4 Monte Carlo codes for different strength magnetic fields and photon beam energies, based on the EGS4 study by Li *et al* (2001) which used input energy spectra

for the 6, 10, 15, 24 and 50 MV photon beams from Mohan *et al* (1985). The photon beam was incident on a $30 \times 30 \times 20$ cm^3 (width $\times$ height $\times$ depth) water phantom with 4×4 cm field size at 100 cm SSD on the surface of the phantom. A slice of uniform transverse magnetic field was applied between 7 and 9 cm depth in the phantom, and the remaining volume outside of this region was set to zero magnetic field. Cylindrical scoring bins of 0.5 cm radius $\times$0.2 cm depth were used to tally the energy deposition from particle interactions. The low-energy electron and photon transport cut-offs were 10 keV and the total number of histories were 10^8 to ensure the statistical uncertainty in each bin did not exceed 2%.

PENELOPE simulations were carried out with identical combinations of magnetic field strength and photon beam energy as those used in the EGS4 study with the exclusion of the 50 MV beam (i.e. Co^{60}, 6, 10, 15 and 24 MV). The PENELOPE simulation parameters, unless otherwise stated, were identical to those used in the EGS4 study (i.e. electron and photon energy cut-offs, number of histories and cylindrical bin volume). Statistical uncertainties of three standard deviations were calculated for each bin. Due to a discrepancy with the EGS4 results for 15 MV and 2 T, the simulations were repeated using photon beam input spectra from Sheikh-Bagheri and Rogers (2002) for 6, 10 and 15 MV beams (24 MV spectrum was not available) to compare with the DPF yields obtained with Mohan *et al* (1985) spectra.

Further PENELOPE simulations were performed with twice the number of scoring bins (i.e. bin depth was halved from 0.2 cm to 0.1 cm depth) to improve the DPF resolution around the magnetic field boundaries where it rapidly increases or decreases. These simulations utilized the Mohan *et al* (1985) photon beam spectra and identical simulation parameters to those used above, apart from a smaller bin volume.

In the course of comparing the current PENELOPE results with the EGS4 results of Li *et al* (2001), a discrepancy persisted for one of the sets of magnetic field and beam energy combinations. As a result, the possibility that the PENELOPE elastic scattering parameters C_1 and C_2 might influence the accuracy of the simulations was also investigated. Limited to the interval of (0,0.2), Salvat *et al* (2003) recommends setting C_1 and C_2 to a conservative value of 0.05 (value adopted in this study), indicating that smaller values would be at the expense of increased simulation time and larger values may cost a loss in accuracy. In this study, the values of C_1 and C_2 inside the region of magnetic field were varied from 0.05 to a value of 0.02, 0.1, 0.2 and 0.5, where $C_1 = C_2$. The influence of electron and photon low-energy transport cut-offs on the DPF was also investigated for 2 and 5 T magnetic fields applied to a 15 MV beam.

Additional simulations, with a 15 MV beam and a 5 T magnetic field, were performed to study any changes in the dose distribution when the 2 cm deep slice of transverse magnetic field applied at different depths in the water phantom (0 to 2 cm, 0.5 to 2.5 cm, 2 to 4 cm, 4 to 6 cm and 7 to 9 cm).

Also included in this paper is a study of the effect of a magnetic field on the distribution of electrons and their radiobiological effectiveness (RBE). PENELOPE simulations were performed to obtain a low-energy (up to 1 MeV) electron spectrum with and without a slice of transverse magnetic field applied between 7 and 9 cm depth. A 15 MV beam and magnetic field strengths of 2 and 5 T were chosen for this study, where the transport parameters were identical to those used previously (i.e. electron and photon transport cut-offs of 10 keV and 10^8 histories). Electrons with an energy less than 1 MeV were binned according to their energy and depth along the central axis using bin intervals of 10 keV and 0.2 cm, respectively. Normalization of the electron spectrum obtained with magnetic field to that obtained without accentuated changes in the electron spectrum that may correspond to alterations in RBE.

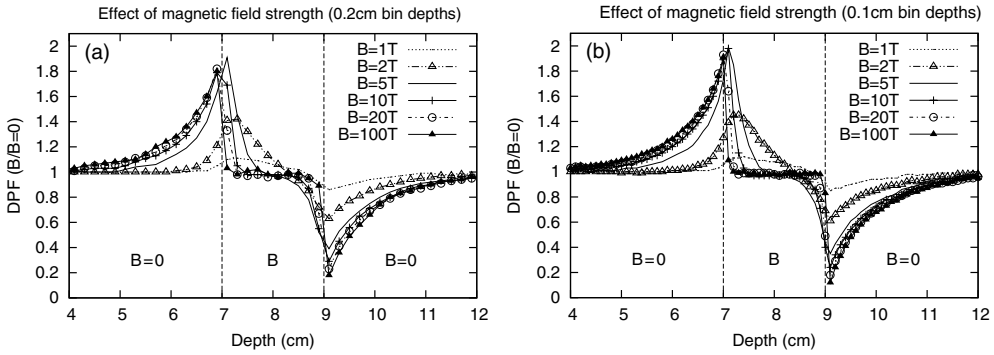

Figure 2. Dose distribution for a 15 MV beam with a slice of transverse magnetic field **B** = 1, 2, 5, 10, 20 and 100 T, using a bin depth of (a) 0.2 cm and (b) 0.1 cm.

Table 1. Comparison of the maximum DPF for a 15 MV beam with **B** = 1 to 100 T.

	EGS4	PENELOPE(Mo)		PENELOPE(SBR)		
B(T)	DPF	DPF	Mo:EGS4	DPF	SBR:EGS4	SBR:Mo
1	1.08	1.11 ± 0.02	1.03	1.11 ± 0.02	1.03	1.00
2	1.67	1.42 ± 0.02	0.85	1.43 ± 0.02	0.86	1.01
2($C = 0.02$)	–	1.41 ± 0.02	–	–	–	–
2($C = 0.1$)	–	1.40 ± 0.02	–	–	–	–
2($C = 0.2$)	–	1.41 ± 0.02	–	–	–	–
2($C = 0.5$)	–	1.41 ± 0.02	–	–	–	–
3	–	1.71 ± 0.03	–	1.73 ± 0.03	–	1.01
4	–	1.87 ± 0.01	–	1.87 ± 0.02	–	1.00
5	1.97	1.91 ± 0.03	0.97	1.92 ± 0.04	0.98	1.01
10	1.81	1.79 ± 0.02	0.99	1.81 ± 0.06	1.00	1.01
20	1.85	1.82 ± 0.05	0.98	1.85 ± 0.06	1.00	1.02
100	–	1.80 ± 0.05	–	–	–	–

3. Results

3.1. Effect of magnetic field strength

The effect of magnetic field strength on a 15 MV beam is presented in figure 2 in a plot of the DPF as a function of depth along the beam's axis. Tables 1 and 2 compare the maximum and minimum DPF obtained with PENELOPE and EGS4 for different strength magnetic fields applied to a 15 MV beam, where PENELOPE(Mo) are the results obtained with Mohan *et al* (1985) spectra and PENELOPE(SBR) are the results obtained with Sheikh-Bagheri and Rogers (2002) spectra. Also included in the tables are the DPF yields obtained with a 2 T field using different elastic scattering values C_1 and C_2 which had no effect on the DPF yields. The largest dose enhancement (91%) was obtained with a magnetic field strength of 5 T which is more than double that obtained with a 2 T field and 8 times larger than that obtained with 1 T. Further increases in field strength failed to yield larger dose enhancements where values of 79%, 82% and 80% were obtained with 10, 20 and 100 T, respectively. Almost all of the PENELOPE DPF results were within 4% of those obtained with EGS4. The

Table 2. Comparison of the minimum DPF for a 15 MV beam with $\mathbf{B} = 1$ to 100 T.

	EGS4	PENELOPE(Mo)		PENELOPE(SBR)		
B(T)	DPF	DPF	Mo:EGS4	DPF	SBR:EGS4	SBR:Mo
1	0.84	0.86 ± 0.01	1.02	0.86 ± 0.01	1.02	1.00
2	0.51	0.63 ± 0.01	1.24	0.63 ± 0.01	1.24	1.00
2($C = 0.02$)	0.51	0.64 ± 0.01	1.25	–	–	–
2($C = 0.1$)	–	0.63 ± 0.01	–	–	–	–
2($C = 0.2$)	–	0.64 ± 0.01	–	–	–	–
2($C = 0.5$)	–	0.64 ± 0.01	–	–	–	–
3	–	0.51 ± 0.01	–	0.50 ± 0.01	–	0.98
4	–	0.44 ± 0.01	–	0.43 ± 0.01	–	0.98
5	0.39	0.39 ± 0.01	1.00	0.39 ± 0.01	1.00	1.00
10	0.28	0.29 ± 0.01	1.04	0.28 ± 0.02	1.00	0.97
20	0.21	0.23 ± 0.05	1.10	0.22 ± 0.05	1.05	0.96
100	–	0.18 ± 0.11	–	–	–	–

Table 3. Comparison of the maximum DPF for a 15 MV beam with $\mathbf{B} = 1$ to 100 T using 0.1 and 0.2 cm bin depths.

	EGS4	PENELOPE(A) (0.2 cm bins)		PENELOPE(B) (0.1 cm bins)		
B(T)	DPF	DPF	PEN(A):EGS4	DPF	PEN(B):EGS4	PEN(B):PEN(A))
1	1.08	1.11 ± 0.02	1.03	1.12 ± 0.03	1.04	1.01
2	1.67	1.42 ± 0.02	0.85	1.45 ± 0.02	0.87	1.02
3	–	1.71 ± 0.03	–	1.73 ± 0.02	–	1.01
4	–	1.87 ± 0.01	–	1.88 ± 0.03	–	1.01
5	1.97	1.91 ± 0.03	0.97	1.99 ± 0.02	1.01	1.04
10	1.81	1.79 ± 0.02	0.99	1.98 ± 0.07	1.09	1.11
20	1.85	1.82 ± 0.05	0.98	1.93 ± 0.03	1.04	1.06
100	–	1.80 ± 0.05	–	1.91 ± 0.14	–	1.06

exceptions were the 2 T maximum DPF and the 2 and 20 T minimum DPF results, yielding respective discrepancies of 24%, 15% and 10% for PENELOPE(Mo), and 24%, 14% and 5% for PENELOPE(SBR). All PENELOPE(Mo) and PENELOPE(SBR) results were within 4% of each other. Decreasing the PENELOPE electron and photon low-energy transport cut-offs from 10 keV to 1 keV had no affect on the DPF results, nor the low-energy spectrum of a 15 MV beam when 2 and 5 T magnetic fields were applied.

Figure 2 shows improved DPF resolution with a smaller bin volume (i.e. 0.1 cm depth), particularly in the dose enhancement and dose reduction regions at the magnetic field boundaries. A comparison of the maximum and minimum DPF yields obtained with PENELOPE and EGS4 are presented in tables 3 and 4, where the results labelled PENELOPE(A) correspond to a bin depth of 0.2 cm (identical bin volume to that used in EGS4) whilst those labelled PENELOPE(B) correspond to a bin depth of 0.1 cm. The ratio of DPF yields for the two different bin volumes (PEN(B):PEN(A)) indicates the smaller 0.1 cm deep bins yield a slightly larger maximum DPF and smaller minimum DPF than the larger 0.2 cm deep bins, where the largest deviations are 11% for the maximum DPF and 33% for the minimum DPF obtained with 10 and 100 T, respectively.

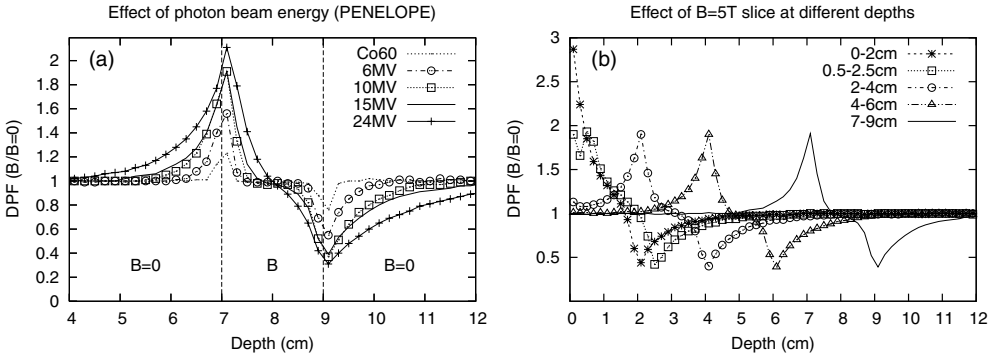

Figure 3. Dose distribution obtained with a slice of 5 T transverse magnetic field applied (a) to different energy photon beams: Co^{60}, 6, 10, 15 and 24 MV (at 7 to 9 cm depth), and (b) at different depths in a water phantom for a 15 MV beam.

Table 4. Comparison of the minimum DPF for a 15 MV beam with $\mathbf{B} = 1$ to 100 T using 0.1 and 0.2 cm bin depths.

	EGS4	PENELOPE(A) (0.2 cm bins)		PENELOPE(B) (0.1 cm bins)		
B(T)	DPF	DPF	PEN(A):EGS4	DPF	PEN(B):EGS4	PEN(B):PEN(A)
1	0.84	0.86 ± 0.01	1.02	0.85 ± 0.01	1.01	0.99
2	0.51	0.63 ± 0.01	1.24	0.61 ± 0.01	1.20	0.97
3	–	0.51 ± 0.01	–	0.48 ± 0.01	–	0.94
4	–	0.44 ± 0.01	–	0.41 ± 0.01	–	0.93
5	0.39	0.39 ± 0.01	1.00	0.35 ± 0.01	0.90	0.90
10	0.28	0.29 ± 0.01	1.04	0.24 ± 0.01	0.86	0.83
20	0.21	0.23 ± 0.05	1.10	0.18 ± 0.03	0.86	0.78
100	–	0.18 ± 0.11	–	0.12 ± 0.11	–	0.67

Table 5. Comparison of the maximum DPF for different photon beams with $\mathbf{B} = 5$ T.

	EGS4	PENELOPE(Mo)		PENELOPE(SBR)		
Beam	DPF	DPF	DPF(Mo:EGS4)	DPF	DPF(SBR:EGS4)	DPF(SBR:Mo)
Co^{60}	1.16	1.23	1.06	1.23	1.06	1.00
6 MV	1.56	1.56	1.00	1.59	1.02	1.02
10 MV	1.82	1.91	1.05	1.85	1.02	0.97
15 MV	1.97	1.91	0.97	1.92	0.98	1.01
24 MV	2.08	2.11	1.01	–	–	–

3.2. Effect of photon beam energy

Figure 3(a) illustrates the dose perturbation effect obtained with a slice of 5 T magnetic field (7 to 9 cm depth) applied to the following photon beams: Co^{60}, 6, 10, 15 and 24 MV. Tables 5 and 6 compares the maximum and minimum DPF yields obtained with PENELOPE and EGS4, where PENELOPE(Mo) and PENELOPE(SBR) are the results obtained with Mohan *et al* (1985) spectra and Sheikh-Bagheri and Rogers (2002) spectra, respectively. The

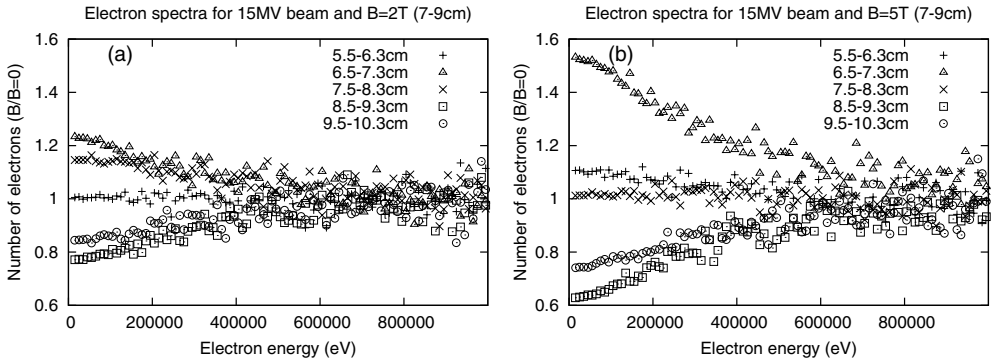

Figure 4. Normalized electron spectra for a 15 MV beam with a slice of transverse magnetic field $\mathbf{B}$ = (a) 2 T, and (b) 5 T.

Table 6. Comparison of the minimum DPF for different photon beams with $\mathbf{B} = 5$ T.

	EGS4	PENELOPE(Mo)		PENELOPE(SBR)		
Beam	DPF	DPF	DPF(Mo:EGS4)	DPF	DPF(SBR:EGS4)	DPF(SBR:Mo)
Co^{60}	0.78	0.76	0.97	0.76	0.97	1.00
6 MV	0.55	0.55	1.00	0.54	0.98	0.98
10 MV	0.44	0.37	0.84	0.41	0.93	1.11
15 MV	0.39	0.39	1.00	0.39	1.00	1.00
24 MV	0.31	0.31	1.00	–	–	–

PENELOPE(Mo) DPF yields were within 6% of those obtained with EGS4, except for the 10 MV minimum DPF which was 16% less than that obtained with EGS4. The majority of PENELOPE(Mo) and PENELOPE(SBR) DPF results were within 3% of each other, where the 10 MV minimum DPF result yielded the largest discrepancy (11%). Repeating the 10 MV PENELOPE simulations with different random seed values had no affect on the minimum DPF result.

The effect of a 5 T magnetic field (2 cm deep) applied to a 15 MV beam at various depths in a water phantom is illustrated in figure 3(b). Positioning the slice of magnetic field just below the phantom's surface (0 to 2 cm) produced a maximum DPF of about 2.85 at the entrance of the phantom. Moving the position of the field from the surface to a depth of 0.5 to 2.5 cm yielded a DPF of 1.9 at the entrance of the phantom, that dropped to 1.65 at 0.3 cm depth before rising again to a maximum DPF of 1.95 at 0.5 cm. Positioning the slice of field beyond these depths did not alter the maximum and minimum DPF yields. The effect of the width of the magnetic field region has also been examined for the above combination of magnetic field and photon beam, investigated with widths of 1 to 4 cm. The result is no variation in the DPF with these widths.

Normalized electron spectra, or the number of electrons obtained with a magnetic field to that obtained without, for a 15 MV beam with 2 and 5 T magnetic fields are presented in figures 4(a) and (b), respectively. In the interest of clarity, the electron spectra have been presented in five 1 cm deep regions as follows: region 1—before the slice of magnetic field (5.5 to 6.5 cm depth); region 2—entering the slice (6.5 to 7.5 cm); region 3—inside the slice (7.5 to 8.5 cm); region 4—exiting the slice (8.5 to 9.5 cm); region 5—beyond the slice

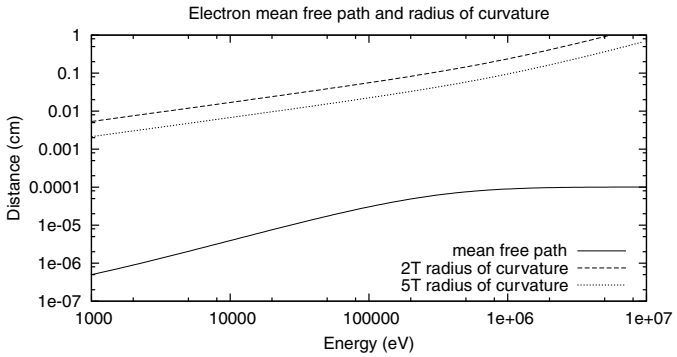

Figure 5. Energy dependence of electron mean free path and radius of curvature in magnetic field.

(9.5 to 10.5 cm). A trend common to both the 2 and 5 T result is an increase in electron yield approaching the slice of magnetic field and a reduction beyond.

4. Discussion

The effect of magnetic field strength on the dose distribution of a 15 MV beam was an increase in the DPF at depths approaching the magnetic field region. The maximum dose perturbation occurred at the field boundary nearest to the surface (∼7 cm depth). The region of dose enhancement was followed by a region of dose reduction, where the DPF dropped rapidly to a minimum value at the furthest magnetic field boundary (∼9 cm depth) and returned to unity at about 12 cm depth.

The region of dose enhancement arises from secondary electrons on average having an initial direction downstream. In the absence of a magnetic field, this leads to dose deposited some distance downstream. The effect of the transverse magnetic field is to reduce the average distance between the depth at which an electron originates and the depth at which most of its energy gets deposited. This could be pictured as due to the electrons spiralling around the transverse magnetic field vector which reduces their depth of interaction and the depth of any secondary particles they produce.

The radius of curvature of an electron subjected to a magnetic field, and its mean free path (in water) between interactions, are both energy dependent as shown in figure 5. As the figure shows, the radius of curvature is several orders of magnitude greater than the mean free path. This might lead to the erroneous conclusion that it is not possible for the magnetic field to influence the dose distribution. It must be remembered however that most electron interactions produce negligible change in the electron trajectory. Therefore, more significant than the mean free path is the mean distance an electron must travel before its trajectory is altered from its original path by one radian. As long as this distance is not significantly smaller than the radius of curvature we expect to see an effect. Alternatively, one could follow the approach of Bielajew, who compared the radius of an electron in a magnetic field to its range, and derived a 'rule of thumb' showing these lengths become comparable in water at a magnetic field strength of approximately two thirds of a Tesla for relativistic energies (Bielajew 1993). Note that this result is independent of electron kinetic energy as both the range and the radius are linearly dependent on kinetic energy for relativistic electrons. This rule of thumb does not

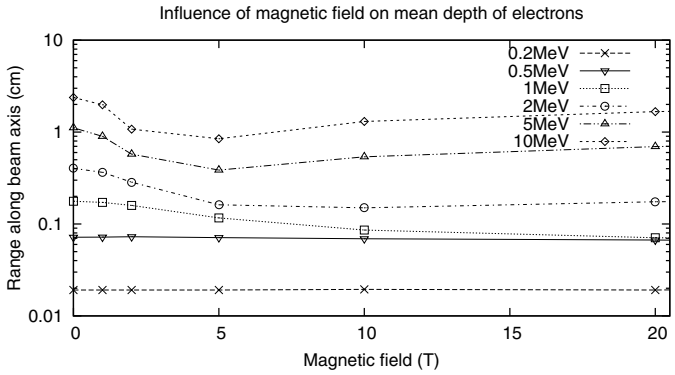

Figure 6. Influence of a magnetic field on the mean distance an electron travels along the beam direction from its origin at 6.9 cm depth.

apply at lower energies where the radius becomes proportional to the square root of the kinetic energy.

This is reflected in figure 6 which shows the mean distance travelled along the beam direction by an electron (for various energies) as a function of magnetic field. It can be seen that electrons with an energy less than 1 MeV are not significantly affected. For a 15 MV photon beam, around 40% of secondary electrons have energies of 1 MeV or higher. Thus, it is primarily these electrons which are responsible for the effects observed. It is also apparent from this figure that magnetic field strengths beyond 5 T will not produce significantly different dose enhancements, since it is at 5 T that the minimum distance an electron travels in the beam direction from its origin is observed.

Consequently, higher energy electrons suffer a greater deviation in their path due to the magnetic field than lower energy electrons, resulting in shallower depths of interaction and production of any secondary particles. This increase in dose at shallower depths gives rise to the dose enhancement observed in the region approaching the magnetic field, where the distribution of particle energies, depths of interaction and ranges gives rise to its breadth.

The largest maximum DPF yield (1.91) occurred with a field strength of 5 T, where stronger magnetic fields failed to yield a larger maximum DPF due to fewer low-energy electrons being able to escape the magnetic field as their radii of curvature have become too confined. This also explains the steep fall-off in the DPF yield between the maximum and minimum value inside the magnetic field region. The region of dose reduction corresponds to the absence of electrons, and any secondary particles they produce, that would otherwise be present in the absence of a magnetic field. Thus, the primary dose contributors in this region are photons (since they are unaffected by the magnetic field) and any secondary particles they produce. The reduction in minimum DPF yield with increasing magnetic field strength is due to fewer electrons escaping the magnetic field since their smaller radii of curvature reduces their depth of interaction.

The PENELOPE elastic scattering parameters C_1 and C_2 had no influence on the results, attributed to the improved modelling of soft energy losses in PENELOPE (Salvat *et al* 2003). Decreasing the PENELOPE electron and photon low-energy transport cut-offs from 10 keV to 1 keV also had no effect on the DPF yield or the low-energy electron spectrum. Doubling the number of scoring bins (by halving their depth) affected the maximum and minimum DPF

yields. The slight enhancement in the maximum DPF with smaller bins is attributed to the improved resolution of the position of maximum DPF, where the largest enhancement (11%) was observed for the 10 T maximum DPF result which shifted from a depth of 6.9 cm to 7.1 cm. Significant enhancements of 6% were also observed for the 20 T and 100 T maximum DPF results where their positions shifted from 6.9 to 7.0 cm depth. The improved bin resolution also had an effect on the minimum DPF yield, where its value decreased with increasing magnetic field but its position (depth) remained fixed at 9.1 cm, despite the additional bin at 9 cm on the field boundary (i.e. 0.2 cm deep bins at 8.9 and 9.1 cm became 8.9, 9 and 9.1 cm bins with 0.1 cm deep bins). This additional bin is responsible for the reduction in the minimum DPF yield as it acquires dose immediately beyond the magnetic field that would otherwise, with 0.2 cm deep bins, be deposited in the 9.1 cm bin. Increasing the magnetic field reduces the radii of curvature of electrons, and consequently their depth of interaction, resulting in fewer electrons escaping the magnetic field which increases the dose on the field boundary and the steepness of the DPF fall-off.

The larger maximum and minimum DPF yields obtained with higher photon beam energies, which were subjected to a 5 T transverse magnetic field, is attributed to the greater depths of interaction of the higher energy photons, and hence, increased electron population in the magnetic field region. Increasing the photon beam energy increases the population of high energy electrons and their probability of escaping the magnetic field region (since they have larger ranges and radii of curvature), which leads to broader regions of dose enhancement and reduction and a less-steep DPF fall-off between them.

The substantial increase in the maximum DPF yield obtained with the 2 cm deep slice of 5 T transverse magnetic field applied at the surface of the phantom is attributed to the large population of low-energy electrons in the 'build-up' region (i.e. distance from the surface to the depth at which maximum dose occurs). For a 15 MV beam with a 4×4 cm^2 field size this distance is about 3 cm. Since the range of these low-energy electrons are only fractions of a centimetre (e.g. range of a 100 keV electron in water is 0.01 cm), a magnetic field applied near the surface will reduce their depth of interaction thereby increasing the DPF yield nearer the surface. This also explains the consistent maximum and minimum DPF yields obtained for magnetic field positions beyond this build-up region. The DPF realized in this study will be greater than those attainable with a more realistic magnetic field distribution as has been shown in the work by Jette (2001).

In the study of the low-energy electron spectrum, the largest low-energy electron population occurred in the region entering the magnetic field (6.5–7.5 cm depth). The magnetic field reduces an electron's depth of interaction, particularly low-energy electrons whose ranges are only a fraction of a centimetre forcing them to deposit their dose locally. This reduces the electron population further downstream, especially in the region exiting the slice (8.5–9.5 cm depth) where the depletion of low-energy electrons is the greatest. Increasing the magnetic field strength from 2 to 5 T, increased the maximum and minimum yield of electrons as more electrons became trapped further upstream, especially immediately inside the magnetic field region. The behaviour of the normalized electron population can be explained from the DPF results in figure 2(a). Inside the magnetic field, in the region 7.5–8.5 cm depth, the normalized electron population is approximately unity for the 5 T result and greater than unity for the 2 T result which can be explained from examining the DPF results. In the 2 T results, the 2 T maximum DPF yield occurs at a depth of 7.3 cm and returns to unity at about 8.3 cm depth, resulting in a normalized low-energy electron population of slightly more than unity inside the magnetic field. Similarly, in the region approaching the magnetic field (5.5–6.5 cm depth), the DPF enhancement observed for 5 T, but not for 2 T, corresponds to the normalized low-energy electron population yield of more than unity for 5 T and unity for 2 T.

The reduction in the low-energy population in the region beyond the magnetic field (9.5–10.5 cm depth) corresponds with the reduction in DPF due to a depletion of electrons in this region.

Figure 4 shows an increase in the relative population of low-energy electrons for the region entering the slice of magnetic field (6.5–7.5 cm depth). Since the LET of electrons increases with decreasing energy, low-energy electrons are primarily responsible for radiation damage and hence the relative biological effectiveness (RBE). Therefore it is possible that the increase in low-energy electron population (in the region 6.5–7.5 cm depth) may correspond to an increase in RBE, and conversely, the reduction in low-energy electron population (in the region exiting the magnetic field, 8.5–9.5 cm depth) may correspond to a reduction of RBE. This alteration in RBE could benefit the treatment of tumours close to radiation-sensitive structures by aligning the region with increased RBE with the tumour volume and the region with reduced RBE with the critical structure.

5. Conclusion

The dose distributions of photon beams are affected by the application of a slice of uniform transverse magnetic field. A region of dose enhancement is produced in the region approaching and entering the slice of magnetic field, followed by a region of dose reduction in the region exiting and beyond the slice. The dose enhancement arises from a reduction in the depth of interaction of electrons, and any secondary particles they produce, as they travel through the transverse magnetic field. The largest maximum DPF (91% enhancement) was observed with 5 T, where further increments in magnetic field strength (up to 100 T) failed to produce a larger maximum DPF yield. The breadth of this dose enhancement region is attributed to the spread of energy, depth of interaction, and range of the electrons. Correspondingly, there is a region of dose reduction immediately beyond the magnetic field slice caused by a deficiency of electrons in this region (since photons are unaffected by the magnetic field). The decreasing minimum DPF yield with increasing magnetic field strength is due to the smaller radii of curvature of electrons, which reduces their depth of interaction and probability of escaping the magnetic field.

The PENELOPE maximum and minimum DPF yields were 91% enhancement and 77% reduction, respectively, which are slightly smaller than the respective Li *et al* (2001) EGS4 results of 97% and 79%. Almost all of the PENELOPE DPF yields were within 4% of those obtained with EGS4, where the minor discrepancies between the codes were not resolved. Reducing the PENELOPE photon and electron low-energy transport cut-off to 1 keV and altering the elastic scattering parameters C_1 and C_2 had no effect on the results. Increasing the bin resolution (by halving the depth of the scoring bins from 0.2 to 0.1 cm) produced a small increase in the maximum DPF yields and a corresponding decrease in the minimum DPF, but did not resolve the discrepancies between the PENELOPE and EGS4 results.

The application of a 5 T magnetic field to different energy photon beams produced larger maximum and minimum DPF yields with increasing beam energy. This is because higher energy photons interact at greater depths, and hence, there is a larger electron population in the magnetic field region. The electron deficiency in the region beyond the magnetic field is responsible for the reduction in the minimum DPF yield which decreased with higher beam energies.

The electron population was largest in the region entering the magnetic field slice and least in the region exiting the slice, a trend similar to that observed with the DPF. The larger maximum and minimum electron populations obtained with 5 T compared with 2 T

are attributed to the smaller radii of curvature of electrons, and hence, reduced their depth of interaction which increased their probability of becoming trapped inside the magnetic field region. Lower-energy energy electrons have a greater LET, and thus, increased radiobiological effectiveness (RBE). Thus, the increase in the low-energy electron population in the region entering the slice of magnetic field may correspond to an increase in the RBE, and conversely, the reduction in low-energy electron population in the region exiting the slice may correspond to a reduction of RBE in that region. This alteration in RBE could benefit the treatment of tumours near to radiation-sensitive organs in order to maximize the damage to the tumour whilst reducing the radiation exposure to the critical structures in the body.

The future direction of this work is to replace the slice of uniform magnetic field with a realistic non-uniform field, such as the field produced by an MRI magnet, to determine whether the alterations in the low-energy electron spectrum associated with the regions of dose enhancement still exist.

References

Bielajew A F 1993 The effect of strong magnetic fields on dose deposition from electron and photon beams *Med. Phys.* **20** 1171–9

Bostick W H 1950 Possible techniques in direct-electron beam tumour therapy *Phys. Rev.* **77** 564–5

Chen Y, Bielajew A F, Litzenberg D W, Moran J M and Becchetti F D 2005 Magnetic confinement of electron and photon radiotherapy dose: a Monte Carlo simulation with a nonuniform longitudinal magnetic field *Med. Phys.* **32** 3810–8

Jette D 2000a Magnetic fields with photon beams: dose calculation using electron multiple scattering theory *Med. Phys.* **27** 1705–16

Jette D 2000b Magnetic fields with photon beams: Monte Carlo calculations for a model magnetic field *Med. Phys.* **27** 2726–38

Jette D 2001 Magnetic fields with photon beams: use of circular current loops *Med. Phys.* **28** 2129–38

Kirkby C, Stanescu T, Rathee S, Carlone M, Murray B and Fallone B G 2008 Patient dosimetry for hybrid MRI-radiotherapy systems *Med. Phys.* **35** 1019–27

Lee M C and Ma C M 2000 Monte Carlo characterization of clinical electron beams in transverse magnetic fields *Phys. Med. Biol.* **45** 2947–67

Li X A, Reiffel L, Chu J and Naqvi S 2001 Conformal photon-beam therapy with transverse magnetic fields: a Monte Carlo study *Med. Phys.* **28** 127–33

Litzenberg D W, Fraass B A M, Shan D L, O'Donnell T W, Roberts D A, Becchetti F D, Bielejew A F and Moran J M 2001 An apparatus for applying strong longitudinal magnetic fields to clinical photon and electron beams *Phys. Med. Biol.* **46** N105–15

Mohan R, Chui C and Lidofsky L 1985 Energy and angular distributions of photons from medical linear accelerators *Med. Phys.* **12** 592–7

Nardi E and Barnea G 1999 Electron beam therapy with transverse magnetic fields *Med. Phys.* **26** 967–73

Nelson W R, Hirayama H and Rogers D W O 1985 The EGS4 code system. http://www.slac.stanford.edu/pubs/slacreports/slac-r-265.html

Paliwal B R, Wiley A L, Wessels B W and Choi M C 1978 Magnetic field modification of electron-beam dose distributions in inhomogeneous media *Med. Phys.* **5** 404–8

Raaijmakers A J E, Raaymakers B W and Lagendijk J J W 2005 Integrating a MRI scanner with a 6 MV radiotherapy accelerator: dose increase at tissue-air interfaces in a lateral magnetic field due to returning electrons *Phys. Med. Biol.* **50** 1363–76

Raaijmakers A J E, Raaymakers B W, van der Meer S and Lagendijk J J W 2007 Integrating a MRI scanner with a 6 MV radiotherapy accelerator: impact of the surface orientation on the entrance and exit dose due to the transverse magnetic field *Phys. Med. Biol.* **52** 929–39

Raaymakers B W, Raaijmakers A J E, Kottee A N T J, Jette D and Lagendijk J J W 2004 Integrating a MRI scanner with a 6 MV radiotherapy accelerator: dose deposition in a transverse magnetic field *Phys. Med. Biol.* **49** 4109–18

Salvat F, Fernandez-Varea J M and Sempau J 2003 *PENELOPE-A Code System for Monte Carlo Simulation of Electron and Photon Transport* (Issy-les-Moulineaux, France: OECD Nuclear Energy Agency)

Sheikh-Bagheri D and Rogers D W O 2002 Monte Carlo calculation of nine megavoltage photon beam spectra using the BEAM code *Med. Phys.* **29** 391–402

Shih C C 1975 High energy electron radiotherapy in a magnetic field *Med. Phys.* **2** 9–13

Whitmire D P and Bernard D L 1977a Magnetic enhancement of electron dose distribution in a phantom *Med. Phys.* **4** 127–31

Whitmire D P and Bernard D L 1977b Magnetic modification of the electron-dose distribution in tissue and lung phantoms *Med. Phys.* **4** 409–17